Isolation of an Unusual Deprotonated Form of *o*-Aminobenzylidene: An Intermediate in the Template Condensation of *o*-Aminobenzaldehyde with Platinum(II)

Mark D. Timken, Robert I. Sheldon, William G. Rohly, and Kristin Bowman Mertes*

Contribution from the Department of Chemistry, University of Kansas, Lawrence, Kansas 66045.
Received September 7, 1979

Abstract: The isolation and characterization of the platinum complex of the dimeric condensate of *o*-aminobenzaldehyde, an intermediate en route to the tetraaza macrocyclic ligand obtained from the tetramerization of *o*-aminobenzaldehyde, are described. Deep purple *cis*-[*N*-(*o*-aminobenzylidene)anthranilaldehydato-*O*,*N*,*N*']chloroplatinum, Pt(AAA)Cl, crystallizes in the space group $P2_1/c$ with unit cell dimensions a = 15.771 (2) Å, b = 6.950 (1) Å, c = 18.718 (3) Å, and β = 121.43 (1)°. The immediate coordination sphere of the platinum consists of two nitrogens and the aldehyde oxygen from the dimerization of *o*-aminobenzaldehyde plus, at the fourth site, a chloride ion. Two different Pt–N bonds of 1.93 (2) and 1.99 (1) Å are observed, the former associated with the terminal amine, along with Pt–O and Pt–Cl bonds of 2.01 (1) and 2.309 (5) Å, respectively. Bond lengths and angles are indicative of electron delocalization within the inner chelate ring of the *o*-aminobenzylidene moiety, a result of the unexpected deprotonated terminal amine. Pt(AAA)Cl further reacts to give the fully closed tetraaza macrocyclic complex.

Introduction

Template synthesis, whereby a metal ion assists in directing the course of a multistep reaction by chelation, has had a far-reaching impact on synthetic chemistry. In the presence of a metal ion, for example, closed-ring macrocyclic systems can be obtained from condensation reactions which, in the absence of metal ion, often result in products bearing little or no resemblance to the macrocycle.

A case in point concerns the condensation of *o*-aminobenzaldehyde. In the absence of a metal, various polycyclic compounds are obtained.[1-4] In the presence of strong mineral acids, the diacid salt of a tetrameric condensate is obtained[2,5,6] for which the equilibrium structures I ⇌ II are suggested.[6] The product in the

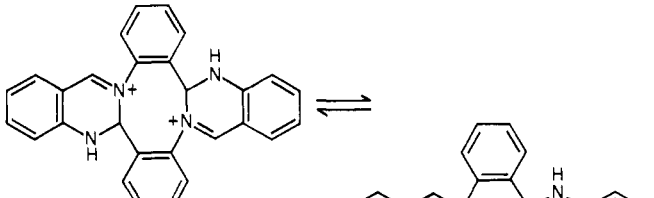

I

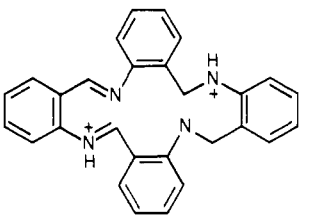

II

presence of a metal ion can be either a tetrameric macrocyclic condensate (III) known as TAAB[7-12] and related to the deprotonated form of II or a trimeric condensate (IV) known as TRI.[7,13]

It has been suggested that the metal ion acts as a Lewis acid catalyst in promoting the formation of the diacid salt and then creates a thermodynamic template effect by stabilizing the formation of II through chelation. Further evidence for a thermodynamic template effect, obtained by Busch and co-workers,[5] is observed upon reaction of various metal acetates with the preformed diacid salt, where only the TAAB and none of the TRI

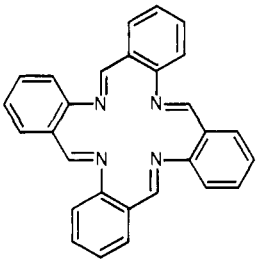

III

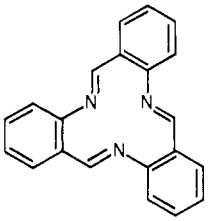

IV

form of the macrocycle is isolated. Such a finding would suggest that outer 16-membered macrocyclic ring bonds of the equilibrium species II remain intact upon condensation.

In a study of the structure–reactivity effects of certain of the second- and third-row transition metals with tetraaza macrocyclic ligands, we attempted the template condensation of *o*-aminobenzaldehyde with palladium(II) and platinum(II).[12] While palladium(II) proceeded smoothly to the $Pd(TAAB)^{2+}$ product, platinum yielded a purple intermediate which then could be reacted further to give $Pt(TAAB)^{2+}$. This paper reports the synthesis and characterization of the purple intermediate in the platinum reaction with *o*-aminobenzaldehyde, a dimeric condensate of *o*-aminobenzaldehyde, henceforth abbreviated Pt(AAA)Cl, which contains the rarely occurring deprotonated *o*-aminobenzylidene chelate ring system.

Experimental Section

Synthesis. All of the chemicals used were reagent grade except those used for spectral measurements where spectral grade solvents were employed. Both *o*-aminobenzaldehyde and the diacid salt were found to react with K_2PtCl_4 to form the purple intermediate. The procedures for each are given in A and B below.

A. Diacid Salt $H_2(TAAB)(BF_4)_2$ (I). Finely ground $H_2(TAAB)(BF_4)_2$ (0.25 g, 0.41 mmol) was added to a solution of K_2PtCl_4 (0.35 g, 0.84 mmol) in 35 mL of water and the mixture was stirred at 35–40 °C for 5 days. The $H_2(TAAB)(BF_4)_2$ did not noticeably dissolve but darkened from a bright red to red-purple as the reaction proceeded. After 5 days the reaction mixture was filtered and the red-purple residue was collected in the filter. The purple product was extracted from the residue by stirring in the absence of heat in about 200 mL of $CHCl_3$. After 8 h of stirring, the mixture was filtered, yielding a deep purple filtrate. Crystals were obtained after slow evaporation of the purple $CHCl_3$ solution and were washed several times with 2–3 mL of $CHCl_3$; yield 16%.

B. *o*-Aminobenzaldehyde. To a hot deaerated solution of 0.25 g (0.6 mmol) of K_2PtCl_4 in 15 mL of H_2O was added dropwise a solution of 0.35 g (2.9 mmol) of *o*-aminobenzaldehyde in a minimum of water to which 2 drops of 6 N HCl had been added. Nitrogen was bubbled through the solution during the reaction because a better crystalline product could be obtained in this manner, although the purple interme-

(1) Seidel, F.; Dick, W. *Ber. Dtsch. Chem. Ges.* **1927**, *60*, 2018-23.
(2) Seidel, F. *Ber. Dtsch. Chem. Ges.* **1926**, *59*, 1894-1908.
(3) Bamberger, E. *Ber. Dtsch. Chem. Ges.* **1927**, *60*, 314-9.
(4) McGeachin, S. G. *Can. J. Chem.* **1966**, *44*, 2323-8.
(5) Skuratowicz, J. S.; Madden, I. L.; Busch, D. H. *Inorg. Chem.* **1977**, *16*, 1721-5.
(6) Goddard, J. D.; Norris, T. *Inorg. Nucl. Chem. Lett.* **1978**, *14*, 211-3.
(7) Melson, G. A.; Busch, D. H. *J. Am. Chem. Soc.* **1964**, *86*, 4830-7.
(8) Cummings, S. C.; Busch, D. H. *Inorg. Chem.* **1971**, *10*, 1220-4.
(9) Taylor, L. T.; Vergaz, S. C.; Busch, D. H. *J. Am. Chem. Soc.* **1966**, *88*, 3170-1.
(10) Takvoryan, N.; Farmery, K.; Katovic, V.; Lovecchio, F. V.; Gore, E. S.; Anderson, L. B.; Busch, D. H. *J. Am. Chem. Soc.* **1974**, *96*, 731-42.
(11) Busch, D. H., et al. *Adv. Chem. Ser.* **1971**, *No. 100*, 44-78.
(12) Brawner, S.; Mertes, K. B. *J. Inorg. Nucl. Chem.* **1979**, *41*, 764-7.
(13) Cummings, S. C.; Busch, D. H. *J. Am. Chem. Soc.* **1970**, *92*, 1924-9.

0002-7863/80/1502-4716$01.00/0

diate could also be isolated in the presence of oxygen. The solution was stirred and heated for 3 h. Upon cooling and filtering of the solution, a purple powder was isolated. Crystals of Pt(AAA)Cl were obtained by dissolving the purple powder in $CHCl_3$, filtering, and slowly evaporating; yield 20%. The crystals decompose noticeably in the atmosphere but can be recrystallized repeatedly from $CHCl_3$. Decomposition can be retarded by storing the crystals at low temperatures in a $CHCl_3$-saturated atmosphere. Anal. Calcd based on 2 N for $PtClON_2C_{14}H_{11}\cdot 0.677CHCl_3$: N, 5.24; C, 32.97; H, 2.20; Cl, 20.09. Found: N, 5.24; C, 33.33; H, 2.15; Cl, 19.06. Analysis was complicated by the volatility of the incorporated $CHCl_3$, which resulted in repeatedly low $CHCl_3$ analyses. Λ_M (Ω^{-1} cm^2 mol^{-1}):[14] CH_2Cl_2, 0.49; DMF, 5.95; CH_3NO_2, 7.29.

Physical Measurements. Infrared spectra from 4000 to 400 cm^{-1} were recorded on a Perkin-Elmer Model 421 grating spectrophotometer as KBr pellets. Mull spectra were not obtained due to color changes of Pt(AAA)Cl in Nujol. Electronic spectra were obtained with 1-cm quartz cells on a Perkin-Elmer Model 555 UV-Vis spectrophotometer in spectrograde $CHCl_3$ and CH_3CN. Molar conductivities for 10^{-3} M solutions were calculated from the electrical resistance obtained with an Industrial Instruments, Inc., Model RC-216B2 conductivity bridge. Elemental analyses for C, H, N, and Cl were performed by Micro-Tech Laboratories.

X-ray Data. Single crystals of Pt(AAA)Cl suitable for X-ray analysis were obtained by slow evaporation of a $CHCl_3$ solution of the complex. Preliminary measurements showed the crystal to belong to the monoclinic space group $P2_1/c$ on the basis of systematic absences $0k0$ ($k \neq 2n$) and $h0l$ ($l \neq 2n$). Unit cell dimensions, determined at −5 °C by an accurate centering of 15 reflections well distributed in reciprocal space, are a = 15.771 (2) Å, b = 6.950 (1) Å, c = 18.718 (3) Å, and β = 121.43 (1)° for Z = 4. The observed density of 2.27 g cm^{-3} obtained by flotation in CCl_4–CH_2I_2 is high for the calculated density of 2.16 g cm^{-3} but could be an effect of the crystal instability.

An initial attempt at data collection at room temperature was thwarted by crystal decay as evidenced by a diminishing of standard reflection intensities by almost 30% within 6 h. A thin plate was then chosen with principal faces $\bar{1}02$, 010, and 100 of dimensions 0.133 × 0.252 × 0.0385 mm, respectively, and mounted for data collection. Data were collected at −5 °C on a Syntex P$\bar{1}$ autodiffractometer fitted with a double-cascade refrigeration system, Model MC-4-84-XR, supplied by FTS Systems, Inc. A takeoff angle of 6.0° was used with nickel-filtered Cu Kα radiation (λ 1.5418 Å). An ω-scan technique, in which seven steps with a total scan range of 0.14° in ω were collected at a scan rate of 0.4°/min, was employed.

Intensities and standard deviations were calculated according to the formulas $I = nrS/60mR$ and $\sigma_I^2 = S(nr/60mR)^2$, where n = the total number of steps, m = the steps used for intensity calculation, R = the scan range, r = the scan rate, and S = the total scan count. The normalized net intensities were calculated by using the consecutive set of three intensities for which the sum was a maximum. For intensities falling in the range from 4000.0 to 35000.0 Hz, coincidence corrections were made according to $I_1 = I_0 + \tau I_0^2$.[15] This is an approximation to the actual Schiff formula for calculation of true intensity values[16] $I_t = I_0 e^{I_t \tau}$, where I_t is the corrected count, I_0 is the observed uncorrected count, and τ is the counter circuit dead time.

Because of the severe decay problems, 21 standard reflections, 3 each along the three principal axes and the four diagonals, were chosen and measured every 300 reflections. Preliminary scans showed background as measured midway between reflection points to be consistently low. Background was not collected during data collection in order to minimize the time required for the collection of a complete data set. Because of the increasingly rapid crystal decay by the end of data collection as well as the low background observed prior to the commencement of data collection, background radiation was neglected. A total of 1349 independent reflections were collected with $2\theta \leq 94°$ of which 1296 had $I \geq 3\sigma(I)$. Lorentz and polarization factors were applied to obtain the structure factors. The decay of the standard reflections at the end of data collection averaged 18.1%. The data were then corrected by the application of a decay correction. At this point the σ_I^2 were also scaled by increasing the σ_I^2 obtained from the counting statistics by $p\sigma_I^2$, where p was chosen as the root-mean-square deviation of the standard reflections, according to Corfield et al.[17] The linear absorption coefficient was calculated to be 234.3 cm^{-1} for $Pt(AAA)Cl\cdot CHCl_3$. Corrections for absorption[18] showed transmission factors to range from 0.0839 to 0.4275. Wilson's method was then used to bring the F^2 to a relatively absolute scale.

Table I. Final Positional and Isotropic Thermal Parameters for Nonhydrogen Atoms in Pt(AAA)Cl[a]

atom	x	y	z	B, Å^2
Pt	0.07916 (6)	−0.01579 (10)	0.35851 (4)	
Cl(1)	0.1336 (4)	−0.0320 (8)	0.4992 (3)	
N(1)	−0.052 (1)	0.020 (2)	0.339 (1)	5.3 (4)
C(1)	−0.139 (2)	−0.007 (2)	0.264 (1)	4.3 (4)
C(2)	−0.229 (2)	−0.005 (2)	0.267 (1)	4.8 (5)
C(3)	−0.321 (2)	−0.036 (3)	0.195 (1)	5.9 (5)
C(4)	−0.323 (2)	−0.068 (3)	0.118 (1)	6.0 (5)
C(5)	−0.241 (2)	−0.069 (3)	0.113 (1)	5.3 (5)
C(6)	−0.145 (2)	−0.036 (2)	0.189 (1)	4.1 (4)
C(7)	−0.062 (2)	−0.033 (2)	0.180 (1)	4.0 (4)
N(2)	0.033 (1)	−0.009 (2)	0.237 (1)	3.9 (4)
C(8)	0.101 (2)	0.014 (2)	0.208 (1)	4.0 (4)
C(9)	0.066 (1)	0.072 (2)	0.124 (1)	4.3 (4)
C(10)	0.127 (2)	0.079 (3)	0.095 (1)	4.8 (4)
C(11)	0.230 (2)	0.028 (3)	0.145 (1)	6.4 (6)
C(12)	0.263 (2)	−0.023 (3)	0.225 (2)	6.9 (6)
C(13)	0.201 (2)	−0.029 (2)	0.259 (1)	4.6 (4)
C(14)	0.250 (2)	−0.064 (3)	0.346 (1)	5.2 (5)
O(1)	0.222 (1)	−0.062 (2)	0.396 (1)	5.3 (3)
C(15)	−0.385 (2)	0.061 (3)	0.412 (1)	
Cl(2)	−0.4285 (6)	0.1752 (15)	0.4044 (5)	
Cl(3)	−0.4370 (6)	0.1295 (16)	0.3064 (8)	
Cl(4)	−0.4455 (7)	0.1862 (19)	0.4494 (4)	

[a] In this table and those subsequent, estimated standard deviations in the least significant figure are given in parentheses.

Solution and Refinement of the Structure. The structure was solved by the heavy-atom method and refined by full-matrix least-squares techniques during which the function $\sum w(|F_o| - |F_c|)^2$ was minimized. Weights used were $1/\sigma_F^2 = 4LpI/\sigma_I^2$. The platinum was located by means of a Patterson synthesis, and a subsequent Fourier map showed the remainder of the nonhydrogen atoms, which included the presence of a $CHCl_3$ solvate molecule. Scattering factor tables from the following sources were used: for platinum, Thomas and Umeda;[19] for carbon, nitrogen, and oxygen, Cromer and Mann;[20] for chlorine and hydrogen, Ibers.[21] Anomalous factors for chlorine and platinum were from Ibers.[21] The $CHCl_3$ chlorides were seen as diffuse ellipsoids of electron density. These were assigned positions taken at the center of the ellipsoid and their thermal parameters were allowed to vary anisotropically, as were those of the platinum and its chloride ligand. Full-matrix least-squares refinement resulted in convergence at R_1 = 0.062 and R_2 = 0.077, where $R_1 = \sum||F_o| - |F_c||/\sum|F_o|$ and $R_2 = \sum w(|F_o| - |F_c|)^2/\sum w|F_o|^2)^{1/2}$. A difference Fourier map at this point showed the presence of regions of electron density corresponding to anticipated hydrogen positions. Although such an occurrence should be highly unlikely because of the large platinum atom, the peaks were indeed evident and argue for the quality of the structure. The hydrogen positions were calculated and assigned temperature factors of $B + 1$, where B is the thermal parameter of the atom to which the hydrogen is attached. Two final cycles of refinement in which hydrogens were included but not refined resulted in convergence at R_1 = 0.059 and R_2 = 0.074. Subsequent refinement in which the thermal parameters of all of the nonhydrogen atoms were varied anisotropically resulted in R_2 = 0.071, a nonsignificant difference according to the Hamilton R test.[22] In the final cycle of refinement, no atom shifted by more than 0.05 of its esd. The estimated standard deviation of an observation of unit weight, given as $\sigma = [\sum w(|F_o| - |F_c|)^2/(N_o - N_v)]^{1/2}$, was 2.74, where N_o = 1296, the number of observed reflections, and N_v = 123, the number of variable parameters. A final difference Fourier map showed residual electron density of 0.95 e/Å^3 in the vicinity of the $CHCl_3$.

Table I contains the final positional and isotropic thermal parameters

(14) Λ_m (Ω^{-1} cm^2 mol^{-1}) for a 1:1 electrolyte is 20–34 for CH_2Cl_2, 65–90 for DMF, and 75–95 for CH_3NO_2 according to: Geary, W. J. *Coord. Chem. Rev.* **1971**, *7*, 81–122. Drago, R. S. *Inorg. Chem.* **1965**, *4*, 840–4. Uguagliatti, P.; Deganello, G.; Busetto, L.; Belluco, U. *Ibid.* **1969**, *8*, 1625–30.

(15) "P2$_1$ Operations Manual"; Syntex Analytical Instrument Co.: Cupertino, CA, 1973.

(16) Friedlander, G.; Kennedy, J. W. "Introduction to Radiochemistry"; Wiley: New York, 1949; p 214.

(17) Corfield, P. W. R.; Doedens, R. J.; Ibers, J. A. *Inorg. Chem.* **1967**, *6*, 197–204.

(18) de Meulenaer, J.; Tompa, H. *Acta Crystallogr.* **1965**, *19*, 1014–8.

(19) Thomas, L. H.; Umeda, K. *J. Chem. Phys.* **1957**, *26*, 293–303.

(20) Cromer, D. T.; Mann, J. B. *Acta Crystallogr., Sect. A* **1968**, *24*, 321–4.

(21) Ibers, J. A. "International Tables for X-ray Crystallography"; Kynoch Press: Birmingham, England, 1968; Vol. III, Tables 3.3.1A and 3.3.2C.

(22) Hamilton, W. C. *Acta Crystallogr.* **1965**, *18*, 502–10.

Table II. Anisotropic Thermal Parameters for Pt(AAA)Cl[a]

atom	β_{11}	β_{22}	β_{33}	β_{12}	β_{13}	β_{23}
Pt	0.00309 (10)	0.01801 (28)	0.00389 (5)	−0.00002 (8)	0.00113 (5)	−0.00033 (6)
C(15)	0.011 (2)	0.031 (7)	0.007 (1)	0.006 (3)	0.004 (1)	−0.003 (2)
Cl(1)	0.0046 (5)	0.0513 (21)	0.0042 (2)	0.0002 (7)	0.0014 (3)	−0.0013 (5)
Cl(2)	0.0132 (8)	0.1074 (45)	0.0104 (5)	−0.0007 (17)	0.0065 (5)	0.0112 (13)
Cl(3)	0.0183 (10)	0.1768 (75)	0.0072 (4)	0.0389 (24)	0.0009 (5)	−0.0112 (14)

[a] Anisotropic thermal parameters are in the form $\exp[-(\beta_{11}h^2 + \beta_{22}k^2 + \beta_{33}l^2 + 2\beta_{12}hk + 2\beta_{13}hl + 2\beta_{23}kl)]$.

Table III. Bond Lengths (Å) and Bond Angles (deg) for Nonhydrogen Atoms in Pt(AAA)Cl

Bond Lengths			
Pt-Cl(1)	2.309 (5)	N(2)-C(8)	1.44 (2)
Pt-N(1)	1.93 (2)	C(8)-C(13)	1.39 (3)
Pt-N(2)	1.99 (1)	C(8)-C(9)	1.43 (2)
Pt-O(1)	2.01 (1)	C(9)-C(10)	1.34 (2)
N(1)-C(1)	1.37 (2)	C(10)-C(11)	1.42 (3)
C(1)-C(6)	1.37 (2)	C(11)-C(12)	1.33 (3)
C(1)-C(2)	1.45 (3)	C(12)-C(13)	1.43 (3)
C(2)-C(3)	1.38 (3)	C(13)-C(14)	1.43 (2)
C(3)-C(4)	1.44 (3)	C(14)-O(1)	1.21 (2)
C(4)-C(5)	1.35 (3)	C(15)-Cl(2)	1.76 (2)
C(5)-C(6)	1.46 (3)	C(15)-Cl(3)	1.76 (2)
C(6)-C(7)	1.40 (2)	C(15)-Cl(4)	1.69 (2)
C(7)-N(2)	1.32 (2)		

Bond Angles			
N(1)-Pt-N(2)	93.6 (7)	C(7)-N(2)-C(8)	118 (2)
N(2)-Pt-O(1)	94.4 (6)	Pt-N(2)-C(8)	122 (1)
O(1)-Pt-Cl(1)	85.1 (4)	N(2)-C(8)-C(9)	120 (2)
Cl(1)-Pt-N(1)	87.0 (5)	N(2)-C(8)-C(13)	122 (2)
Pt-N(1)-C(1)	125 (1)	C(13)-C(8)-C(9)	117 (2)
N(1)-C(1)-C(6)	125 (2)	C(8)-C(9)-C(10)	121 (2)
N(1)-C(1)-C(2)	116 (2)	C(9)-C(10)-C(11)	123 (2)
C(6)-C(1)-C(2)	119 (2)	C(10)-C(11)-C(12)	117 (2)
C(1)-C(2)-C(3)	121 (2)	C(11)-C(12)-C(13)	123 (2)
C(2)-C(3)-C(4)	117 (2)	C(12)-C(13)-C(14)	117 (2)
C(3)-C(4)-C(5)	124 (2)	C(12)-C(13)-C(8)	119 (2)
C(4)-C(5)-C(6)	118 (2)	C(8)-C(13)-C(14)	124 (2)
C(5)-C(6)-C(7)	116 (2)	C(13)-C(14)-O(1)	133 (2)
C(1)-C(6)-C(7)	123 (2)	C(14)-O(1)-Pt	122 (1)
C(5)-C(6)-C(1)	121 (2)	Cl(2)-C(15)-Cl(3)	103 (1)
C(6)-C(7)-N(2)	130 (2)	Cl(2)-C(15)-Cl(4)	104 (2)
C(7)-N(2)-Pt	120 (1)	Cl(3)-C(15)-Cl(4)	107 (1)

Table V. Positional and Thermal Parameters for Hydrogen Atoms in Pt(AAA)Cl

atom	x	y	z	B, Å^2
HN(1)	−0.080	−0.020	0.377	6.21
HC(2)	−0.230	0.000	0.320	5.86
HC(3)	−0.382	−0.045	0.196	6.96
HC(4)	−0.390	−0.080	0.071	6.71
HC(5)	−0.240	−0.075	0.060	6.62
HC(7)	−0.062	−0.045	0.128	5.23
HC(9)	−0.008	0.085	0.097	5.13
HC(10)	0.120	0.091	0.042	5.87
HC(11)	0.245	0.040	0.100	7.31
HC(12)	0.330	−0.030	0.277	8.21
HC(14)	0.325	−0.077	0.377	6.26

and Table II lists the anisotropic thermal parameters for nonhydrogen atoms. Bond lengths and angles are listed in Table III. A list of observed and calculated structure factors is available as supplementary material. Hydrogen atom positional and thermal parameters are given in Table V and hydrogen bond lengths are shown in Table VI.

Results and Discussion

Various physical methods were used to identify the purple crystalline product, including solution conductivities, infrared spectroscopy, and X-ray crystallographic techniques. Sparing solubilities in $CHCl_3$ and decomposition in a variety of other solvents made NMR measurements inaccessible. The product has been confirmed to be the coordinated dimeric condensate of *o*-aminobenzaldehyde and is properly named *cis*-[*N*-(*o*-aminobenzylidene)anthranilaldehydato-*O*,*N*,*N*']chloroplatinum (Pt(AAA)Cl).

Molecular Structure of Pt(AAA)Cl. The numbering scheme is depicted in Figure 1. The immediate coordination sphere of

Table VI. Hydrogen Atom Distances (Å) in Pt(AAA)Cl

HN(1)-N(1)	1.05	HC(9)-C(9)	1.00
HC(2)-C(2)	1.00	HC(10)-C(10)	0.93
HC(3)-C(3)	0.97	HC(11)-C(11)	0.98
HC(4)-C(4)	0.96	HC(12)-C(12)	1.01
HC(5)-C(5)	1.00	HC(14)-C(14)	1.01
HC(7)-C(7)	0.98		

Table VII. Selected Mean Plane Calculations for Pt(AAA)Cl

atom	displacement	atom	displacement
A. Cl(1)-O(1)-N(1)-N(2)			
$-0.1337x - 0.9887y - 0.0682z = 0.0434$			
Pt	−0.0255	C(6)	0.5477
Cl(1)[a]	0.0012	C(7)	0.3545
O(1)[a]	−0.0012	C(8)	−0.3121
N(1)[a]	−0.0012	C(13)	−0.2109
N(2)[a]	0.0012	C(14)	−0.0537
C(1)	0.3525		
B. C(1)-C(2)-C(3)-C(4)-C(5)-C(6)			
$-0.0052x + 0.9840y - 0.1782z = -0.7673$			
C(1)[a]	−0.0069	C(4)[a]	−0.0023
C(2)[a]	0.0014	C(5)[a]	−0.0030
C(3)[a]	0.0030	C(6)[a]	0.0077
C. C(8)-C(9)-C(10)-C(11)-C(12)-C(13)			
$-0.0774x - 0.9546y - 0.2877z = -1.0312$			
C(8)[a]	0.0112	C(11)[a]	0.0077
C(9)[a]	0.0009	C(12)[a]	0.0041
C(10)[a]	−0.0104	C(13)[a]	−0.0136

[a] Atoms used in the least-squares plane calculation.

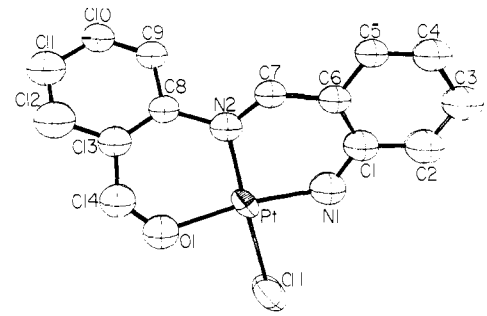

Figure 1. Perspective view of Pt(AAA)Cl showing thermal ellipsoids of 50% probability.

the platinum is square planar. Three of the sites are occupied by the two nitrogens and oxygen of the dimeric condensate with N(1)–Pt–N(2) and N(2)–Pt–O(1) of 93.6 (7) and 94.4 (6)°, respectively. A chloride resides at the fourth site with Cl(1)–Pt–O(1) of 85.1 (4)° and Cl(1)–Pt–N(1) of 87.0 (5)°. The platinum shows little displacement (−0.02 Å) from the N_2OCl plane. With the exception of the phenyl groups, the rest of the molecule deviates considerably from planarity, as can be seen in Table VII which contains some selected mean plane calculations. The two chelate rings are canted as evidenced by the dihedral angles C(6)–C(7)–N(2)–C(8) and C(7)–N(2)–C(8)–C(13) of 172 (2) and 156 (2)°, respectively. Both solution conductivities, which indicated nonelectrolyte behavior in DMF, CH_3NO_2, and CH_2Cl_2, and the absence of a free chloride ion in the electron density maps confirm the presence of the rarely occurring deprotonated *o*-aminobenzylidene moiety.

Molecules related by the inversion center are situated in such

Table VIII. Infrared Spectral Data in the Region 1700–1500 cm^{-1}

$Pt(TAAB)^{2+}$ [a]	assignt	Ni(amben)[b]	assignt	Pt(AAA)Cl	assignt
1603 vs[c]	aromatic	1617 s	C=N	1621 vs	C=O
1587 vs	aromatic	1593 s	conjugated ring interactions	1592 s 1565 m 1546 m	aromatic and conjugated ring interactions
1567 vs	C=N	1537 s	aromatic	1529 s	C=N

[a] Reference 12. [b] Reference 26. [c] Abbreviations used: vs, very strong; s, strong; m, medium.

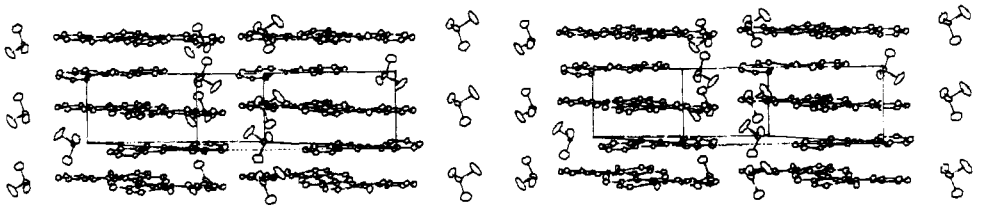

Figure 2. Stereoscopic packing diagram for Pt(AAA)Cl as viewed down the *x* axis with the *z* axis horizontal and the *y* axis vertical. Thermal ellipsoids are shown for 30% probability.

a manner as to suggest the possibility of an N(1)–H···Cl(1)′ interaction. The N(1)–Cl(1)′ distance of 3.86 Å compared to a range of (3.16–3.26) ± 7 Å for N–H···Cl hydrogen bonding,[23] however, indicates that no real interaction exists. Successive molecular layers are packed at intervals of 3.47 Å along the *y* axis. A linear array of metal atoms is not observed; instead, the closest intramolecular nonhydrogen relationship to the platinum within the layers is C(7) at 3.41 (2) Å. The chloroform of crystallization is located between adjacent molecules, within molecular layers.

While the Pt–Cl(1) bond of 2.307 (6) Å is in good agreement with other Pt–Cl bonds, as in *cis*-$Pt(NH_3)_2Cl_2$, where Pt–Cl = 2.33 (1) Å,[24] bond lengths and angles within the dimeric condensate show some interesting effects of the deprotonated *o*-aminobenzylidene. A relatively short Pt–N(1) distance of 1.93 (2) Å is observed (although still within the range observed for platinum(II)) compared to the Pt–N(2) distance of 1.99 (1) Å. The differing lengths, along with a shortened N(1)–C(1) bond of 1.37 (2) Å (compared to 1.48 (1) Å anticipated for R_2C–NH_2[25]), are characteristic of the deprotonated *o*-aminobenzylidene moiety and are observed for a related nickel complex (VA), where the two analogous Ni–N bonds are 1.860 (6) and 1.923 (7) Å.[26,27]

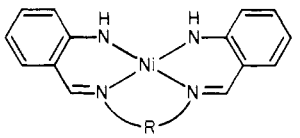

VA, R = $(CH_2)_3$, Ni(ambtn)
B, R = $(CH_2)_2$, Ni(amben)

Within the deprotonated *o*-aminobenzylidene ring, bond lengths indicate lessened aromaticity in the phenyl ring and increased delocalization for the inner chelate ring. Unfortunately, standard deviations are large; however, the regularity of the long–short C–C bond alternation within the phenyl group and the chemical sense emphasize the probable reality of the effect. Although in the related Ni(ambtn) (VA) complex double-bond localization in the phenyl rings is not observed,[26] in the recently reported structure of another condensate of *o*-aminobenzaldehyde the effect is noted.[28] The nickel complex of the tetraaza macrocycle obtained from the template condensation of four *o*-aminobenzaldehyde molecules, TAAB (IV), reacts with two molecules of the enolate of acetone. Two of the four azomethine carbons of the macrocycle are nucleophilically attacked, with adduct formation resulting in two saturated C–N linkages and increased electron delocalization in the remaining two chelate rings. These latter ring systems can be considered to be electronically analogous to that of the deprotonated *o*-aminobenzylidene. A comparison of the bond lengths for Ni(ambtn) (VI),[26] the TAAB adduct (VII),[28] and Pt(AAA)Cl (VIII) follows.

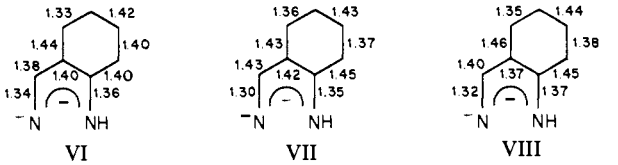

VI VII VIII

As can be seen for all three ring systems, increased delocalization within the inner chelate ring is evident, whereas only the TAAB complex and Pt(AAA)Cl show decreased aromaticity in the phenyl ring. A similar effect is seen in the benzo group of the anthranilaldehydato chelate ring system in Pt(AAA)Cl without delocalization in the inner chelate ring as evidenced by the single-bond character of N(2)–C(8), 1.44 (2) Å, and a short C(14)–O(1) distance, 1.21 (2) Å. The latter reasonably compares with the 1.23-Å[29] C=O bond in a salicylaldehyde complex of Co(II). Angles within both the phenyl and inner chelate ring systems are as expected and compare favorably with the related systems.[26,28]

Spectral Data. The infrared spectrum of Pt(AAA)Cl differs considerably from that of $Pt(TAAB)^{2+}$, the fully closed macrocyclic condensation product. Both N–H and C–H vibrations are observed for the former at 3315 and 2915 cm^{-1}, respectively. The region from 1700 to 1500 cm^{-1} which encompasses phenyl ring, C=N, C=O, and possibly N–H vibrations is particularly diagnostic. Table VIII lists the infrared bands for several related complexes along with some previously reported assignments in the aforementioned region. $[Pt(TAAB)][Cl]_2$, Ni(amben) (VB), and Pt(AAA)Cl are included. Assignment of the band at 1621 cm^{-1} in Pt(AAA)Cl to the C=O stretch can be made with reasonable assurance in view of previous studies of coordinated square-planar unsubstituted salicylaldehyde complexes in which the C=O stretch is observed from 1640 to 1610 cm^{-1}, depending on the metal ion.[30] As is evident from the table, however, ambiguity occurs in assigning the C=N stretching frequency. The assignment has previously been made for TAAB on the basis of spectral changes upon electronic modification of the ligand system. When two of the TAAB chelate rings undergo nucleophilic attack, electron delocalization throughout the remaining two rings occurs and the band at 1567 cm^{-1} shifts to lower energies (~1530 cm^{-1}).[31] A similar effect occurs with ligand reduction of TAAB com-

(23) Ondik, H.; Smith, D. "International Tables for X-ray Crystallography"; Kynoch Press: Birmingham, England, 1968; Vol. III, Table 4.1.12.
(24) Milburn, G. H. W.; Truter, M. R. *J. Chem. Soc. A* **1966**, 1609–16.
(25) Kennard, O. "International Tables for X-ray Crystallography"; Kynoch Press: Birmingham, England, 1968; Vol. III, Table 4.2.4.
(26) Bailey, N. A.; McKenzie, E. D.; Worthington, J. M. *J. Chem. Soc., Dalton Trans.* **1974**, 1363–6.
(27) Green, M.; Tasker, P. A. *J. Chem. Soc. A* **1970**, 2531–9.
(28) Kamenar, B.; Kaitner, B.; Katovic, V.; Busch, D. H. *Inorg. Chem.* **1979**, *18*, 815–8.
(29) Pfluger, C. E.; Hon, P. K.; Harlow, R. L. *J. Cryst. Mol. Struct.* **1974**, 4, 55–61.
(30) Percy, G. C.; Thornton, D. A. *J. Inorg. Nucl. Chem.* **1973**, *35*, 2719–26.
(31) Melson, G. A.; Busch, D. H. *J. Am. Chem. Soc.* **1964**, *86*, 4834–7.
(32) Katovic, V.; Taylor, L. T.; Urbach, F. L.; White, W. H.; Busch, D. H. *Inorg. Chem.* **1972**, *11*, 479–83.

Scheme I

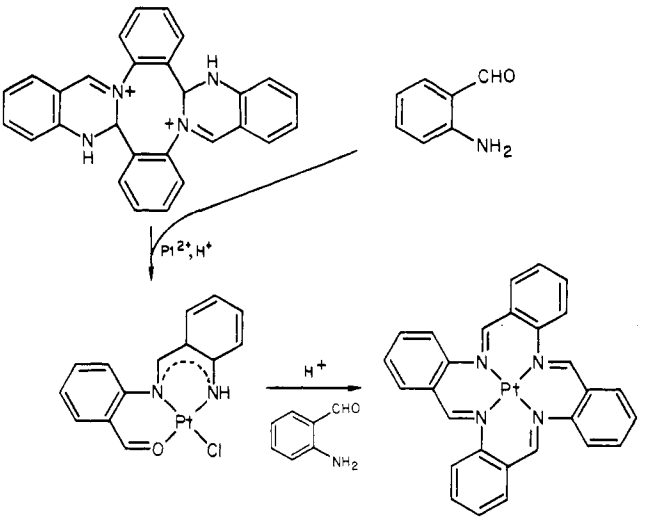

plexes.[32] Such a shift would be anticipated with an increase in electron delocalization which would affect the C=N bond order. The band at 1529 cm^{-1} thus has been assigned on the basis of these observations to the C=N stretching vibration rather than one of the higher energy bands. Of the remaining bands, two possible assignments are available: the N-H deformation vibration, normally occurring between 1650 and 1550 cm^{-1}, and the phenyl ring vibrations, from 1650 to 1450 cm^{-1}. The former are often hidden by the strong phenyl absorptions and are noted to be weak in secondary amines and iminato-like species.[33] As a consequence, the remaining medium to strong bands are most probably related to aromatic absorptions as well as phenyl ring conjugation with C=N and C=O, known to produce enhancement of the ring vibration intensities.[33]

The UV-Vis absorption spectrum of Pt(AAA)Cl consists of a series of intense bands and shoulders throughout both regions. In $CHCl_3$ two bands are observed at 17 300 and 29 900 cm^{-1} with extinction coefficients of 14 200 and 9840, respectively. Shoulders occur at 18 100, 24 300, 26 900, 36 000, and 37 600 cm^{-1}. The origin of these bands is most probably related to metal to ligand charge transfer or to ligand transitions in view of the intensities involved. Similar intense visible bands are observed in complexes of the reduced TAAB ligand as well as in nucleophilic adducts of TAAB where electron delocalization throughout the chelate rings leads to highly chromophoric species.[10,34]

The intermediate nature of Pt(AAA)Cl is confirmed by experiments in which concentrated solutions of the purple crystals in acetonitrile are reacted with *o*-aminobenzaldehyde. Upon acidification the intense bands in the visible region immediately disappear. UV-Vis spectra recorded after heating and stirring of the solution for 1 day are identical with that of $Pt(TAAB)^{2+}$. The total reaction sequence can therefore be described as shown in Scheme I. The mechanistic implications of the presence of the deprotonated *o*-aminobenzylidene moiety, at least in the platinum system, are being investigated.

This is, to our knowledge, the first isolated intermediate in the self-condensation of *o*-aminobenzaldehyde to give transition-metal complexes of the fully cyclized ligand. It forms readily from either *o*-aminobenzaldehyde or the diacid salt in the presence or absence of light or oxygen. The formation of the deprotonated *o*-aminobenzylidene moiety is particularly interesting in view of its rarity. The complex further reacts with a variety of amines, and the products are currently being investigated in order to provide convenient routes to novel polydentate and macrocyclic ligand systems.

Acknowledgments. The authors thank Professor B. K. Lee for use of his diffractometer, for the low-temperature data collection, and for many helpful discussions. K.B.M. acknowledges the donors of the Petroleum Research Fund, administered by the American Chemical Society, and the University of Kansas general research allocation No. 3227-XO-0038 for support of this research.

Supplementary Material Available: A list of observed and calculated structure factors (Table IV) (8 pages). Ordering information is given on any current masthead page.

(33) Bellamy, L. J. "The Infra-red Spectra of Complex Molecules"; Wiley: New York, pp 71-5 and 255-7.

(34) Katovic, V.; Taylor, L. T.; Busch, D. H. *J. Am. Chem. Soc.* **1969**, *91*, 2122-3.

An Inelastic Electron-Tunneling Spectroscopic Study of $Ru_3(CO)_{12}$ Adsorbed on an Aluminum Oxide Surface

W. M. Bowser and W. H. Weinberg*

Contribution from the Division of Chemistry and Chemical Engineering, California Institute of Technology, Pasadena, California 91125. *Received February 14, 1980*

Abstract: The adsorption of $Ru_3(CO)_{12}$ on aluminum oxide has been studied by means of inelastic electron-tunneling spectroscopy. The complex was found to retain its molecular structure when adsorbed on a hydroxylated alumina surface at low temperature. Upon heating the surface to 470 K in 0.1 torr of O_2, the $Ru_3(CO)_{12}$ is lost from it through desorption and possible oxidation of the complex.

Introduction

In the area of chemisorption and heterogeneous catalysis, one of the more technologically important fields of study is research aimed at understanding the properties of supported metal catalysts on a molecular level. A rather new technique, ideally suited for the investigation of such systems, is inelastic electron-tunneling spectroscopy (IETS).[1-3] IETS provides vibrational information concerning the support-supported metal-adsorbate system. In this sense, IETS is analogous to IR spectroscopy. Tunneling spectroscopy, however, has several advantages over IR spectroscopy; for example: (1) IETS is sensitive to both infrared (dipolar) and Raman (induced dipolar) active excitations; (2) the IETS sample is a planar surface with an area on the order of 1 mm^2,

(1) W. H. Weinberg, *Annu. Rev. Phys. Chem.*, **29**, 115 (1978).

(2) P. K. Hansma, *Phys. Rep.*, **30**, 145 (1977).

(3) T. Wolfram, Ed., "Inelastic Electron Tunneling Spectroscopy", Springer-Verlag, New York, 1978.

0002-7863/80/1502-4720$01.00/0